Available online at www.sciencedirect.com
ScienceDirect
Journal of Sound and Vibration 314 (2008) 867–884
JOURNAL OF SOUND AND VIBRATION
www.elsevier.com/locate/jsvi

Beamforming-based partial field decomposition in NAH

Yeon June Kang*, Eui Seok Hwang

Advanced Automotive Research Center, Institute of Advanced Machinery Design, School of Mechanical and Aerospace Engineering, Seoul National University, Gwanangno 599, Shinlim-9Dong Kwanak-Gu, Seoul 151-744, Korea

Received 8 March 2007; received in revised form 28 September 2007; accepted 5 January 2008
Handling Editor: L.G. Tham
Available online 12 February 2008

Abstract

In this paper, a methodology for partial field decomposition is presented that is based on the beamforming algorithm for the application of acoustical holography to the composite sound fields generated by multiple incoherent sound sources. The unique aspect of the method is the use of estimated source signals identified via beamforming as reference source signals in the decomposition procedure. Numerical simulations are performed with particular emphasis on the robustness of the proposed technique under various situations. The experimental results show that the method identifies source signals very effectively regardless of the distance from source to reference and also has potential for use in distributed sources.

1. Introduction

Among the many ways of identifying noise sources and transmission paths, acoustical holography is one of the most powerful tools available for reconstructing and visualizing acoustical quantities. In the early 1980s, Williams and Maynard et al. developed the Near-field Acoustical Holography (NAH) method based on a two-dimensional spatial FFT algorithm [1]. NAH can reconstruct high resolution source images by including evanescent waves that are neglected in conventional acoustical holography methods. NAH can also provide complete information on the acoustical quantities in any region merely by measuring the acoustic pressures on the surface surrounding the region in question.

NAH is based on spatial wave number decomposition, which requires measurement of a sound field in order to obtain information on the spatial distributions of relative phases. If the sound field is fully coherent, this can easily be achieved by scanning with one field microphone and one reference microphone. However, in many practical cases, the sound field is generated by a combination of incoherent or partially coherent sources. In order to apply NAH, such a composite sound field must be decomposed into a set of fully coherent partial sound fields. Then, NAH can be applied to each coherent partial field separately, and their individual contributions can be projected and combined on a new plane of interest.

To identify partial fields, the Singular Value Decomposition (SVD) method [2] and the Partial Coherence method [3,4] have attracted much attention due to their success in many practical applications. These two

*Corresponding author. Tel.: +82 2 880 1691; fax: +82 2 883 1513.
E-mail address: yeonjune@snu.ac.kr (Y.J. Kang).

0022-460X/$ - see front matter
doi:10.1016/j.jsv.2008.01.010

methods have been extensively studied [5–7] and applied to real-world problems [8,9]. However, they have an inevitable drawback in that they require a reference microphone to be placed close to each source although exact source locations are often not known. Especially, their performance deteriorates drastically as the distance between a reference microphone and the corresponding source increases. Those methods are briefly summarized in Appendices A and B.

In this paper, an alternative method based on the beamforming algorithm whose performance degrades much more slowly as the distance between source and reference microphone increases is proposed. In sensor array signal processing, a number of algorithms have been proposed for the identification of multiple incoherent sources. A Multiple Signal Classification (MUSIC) method based on the eigen-characterization of the cross-spectral matrix is one of the most promising and widely used algorithms [7,10]. In acoustical applications, Bai [11] employed the MUSIC algorithm to identify industrial noise sources from far-field measurements.

In the method proposed here, the MUSIC algorithm is adapted to determine the locations of source candidates in the near-field. Then, the source signals are estimated using a beam steering vector in such a way that the directional component of the source signal of interest is maintained while those of the other source signals are minimized or removed from the measured reference signals. Since beamforming is suitable for point sources or far-field problems, a modified beam vector that considers several points of the area is applied to distributed sources in near-field applications in order to maintain the desired source signal or to suppress undesired source signals.

Once the signals have been estimated, the partial fields are reconstructed by estimating the transfer functions between the estimated source signals and the field microphone measurements. Since the source signals are available, the problem of estimating the transfer functions reduces to a deterministic least squares problem. Numerical simulation confirms the performance of the proposed method under various conditions. In order to show the potential for applying the proposed method to distributed sources, experiments with two distributed sources are conducted, which clearly show its extensibility to distributed sources. It should be noted that the proposed procedure may be considered to be an experimental alternative to other recently proposed procedures in which virtual references are placed close to candidate source locations in a post-processing step [12–14]. The present procedure may be an effective alternative to the virtual reference method if for any reason it is difficult to position virtual references close to the source.

Section 2 introduces briefly the merits of the proposed method as compared with existing approaches to partial field decomposition. Next, the proposed alternative method based on beamforming is described. In Section 3, the performance of the beamforming procedure is analyzed through computer simulations. Section 4 describes experimental results along with a discussion of the results. Throughout the analysis in Sections 3 and 4, the performance of the proposed algorithm is compared to those of existing algorithms, in particular to the SVD and partial coherence methods.

2. Theory

Conventional methods decompose a composite field into partial fields by utilizing the statistical properties of selected reference signals. Assuming incoherent sources, a reference microphone should be kept as close as possible to each source in order to mitigate crosstalk between source signals. This is essential for high fidelity reproduction of partial fields. However, in many practical applications, it is difficult to locate a reference microphone near each source, because for this to be possible the partial field decomposition algorithm must be robust with regard to the locations of reference microphones if it is to be effective in a wide variety of applications.

In this section, an alternative approach based on beamforming is proposed in order to overcome the limitations of the conventional approaches. The locations of sources are estimated via the MUSIC algorithm. The source signals are then estimated by computing the weighted sums of the reference signals in such a way that each weighted sum may emphasize a specific source signal while suppressing the contributions of the rest of the source signals. The partial fields are reconstructed by calculating the transfer functions between the estimated source signals and the field microphone measurements in a deterministic manner.

2.1. Source localization via MUSIC algorithm

Consider a linear array of M reference microphones that receive signals from N incoherent sources. The measured reference signals can be expressed in the frequency domain as a linear combination of the N signals and noise: i.e.,

$$r_j = \sum_{i=1}^{N} g_{ji} s_i + n_j, \tag{1}$$

where r_j denotes the discrete Fourier transform of the jth reference signal, s_i denotes the ith source signal and g_{ij} denotes the transfer function between r_j and s_i defined as

$$g_{ji} = \frac{\mathrm{e}^{-\mathrm{j}kl_{ji}}}{l_{ji}}, \tag{2}$$

where $\mathrm{j} = \sqrt{-1}$ and l_{ji} is a distance between r_j and s_i. Here n_j denotes white Gaussian noise and

$$E(n_i, n_j) = \sigma_n^2 \delta(i-j), \tag{3}$$

where

$$\delta(i-j) = \begin{cases} 1 & \text{when } i = j, \\ 0 & \text{otherwise.} \end{cases} \tag{4}$$

In vector–matrix form, Eq. (1) becomes

$$\mathbf{r} = \begin{bmatrix} r_1 \\ \\ r_M \end{bmatrix} = \begin{bmatrix} \mathbf{g}_1 \, \mathbf{g}_2 \cdots \mathbf{g}_{N-1} \, \mathbf{g}_N \end{bmatrix} \begin{bmatrix} s_1 \\ \\ s_N \end{bmatrix} + \begin{bmatrix} n_1 \\ \\ n_M \end{bmatrix} = \mathbf{G}\mathbf{s} + \mathbf{n}, \tag{5}$$

where $\mathbf{r}$ is a vector representing the finite Fourier transform of the reference signals, $\mathbf{G}$ is a transfer matrix whose elements are $\mathbf{g}_i = [g_{1i} \quad g_{2i} \quad \ldots \quad g_{\mathrm{M}i}]^{\mathrm{T}}$, $\mathbf{s}$ is a vector which represents the source signals, and $\mathbf{n}$ is a measurement noise vector. The cross-spectral matrix of the references $\mathbf{S}_{rr}$ can then be written as

$$\mathbf{S}_{rr} = \mathrm{E}[\mathbf{r}\mathbf{r}^H] = \mathbf{G}\mathrm{E}[\mathbf{s}\mathbf{s}^H]\mathbf{G}^H + \mathrm{E}[\mathbf{n}\mathbf{n}^H] = \mathbf{G}\mathbf{S}_{ss}\mathbf{G}^H + \sigma_n^2\mathbf{I}, \tag{6}$$

where the notation $\mathrm{E}[\cdot]$ is the expectation factor, $\mathbf{S}_{ss}$ denotes the cross-spectral matrix of the source signals $\mathrm{E}[\mathbf{s}\mathbf{s}^H]$, and $\mathbf{G}^H$ is the Hermitian transpose of $\mathbf{G}$.

Eigen decomposition of the reference cross-spectral matrix $\mathbf{S}_{rr}$ can be expressed as

$$\mathbf{S}_{rr} = \sum_{i=1}^{M} \lambda_i \mathbf{v}_i \mathbf{v}_i^H, \tag{7}$$

where $\mathbf{v}_i$ is the ith eigenvector, and

$$\lambda_i = \begin{cases} \mu_i + \sigma_n^2, & i = 1, 2, \ldots, N, \\ \sigma_n^2, & i = N+1, N+2, \ldots, M. \end{cases} \tag{8}$$

Here, $\mu_1 \geqslant \mu_2 \geqslant \cdots \geqslant \mu_N$ denote the eigenvalues of the cross-spectral matrix of the source signals, and σ_n^2 is the variance of noise. The above equations imply that the eigenvalues and the associated eigenvectors of the reference cross-spectral matrix can be subdivided into two groups. One group spans the source signals vector and the noise components that are indistinguishable from the source signals, while the other spans the remaining noise components [7,11,15]. Consider a vector $\hat{\mathbf{g}}_i$ such that

$$\hat{\mathbf{g}}_i = [\,\hat{g}_{1i} \quad \hat{g}_{2i} \quad \cdots \quad \hat{g}_{Mi}\,]^{\mathrm{T}}, \tag{9}$$

where g_{ji} is Green's function between the jth reference microphone and ith source. The vector represents the array response vector of the ith source. After some algebraic manipulation, it can be shown that

$$\mathbf{v}_j^H \hat{\mathbf{g}}_i = 0 \quad \text{for} \quad 1 \leqslant i \leqslant N, N+1 \leqslant j \leqslant M, \tag{10}$$

where $\mathbf{v}_{N+1},\ldots,\mathbf{v}_M$ are the eigenvectors of the reference cross-spectral matrix corresponding to noise. Eq. (10) represents the orthogonal properties of the noise subspace and the source signal. The proof of Eq. (10) is provided in Ref. [14]. The MUSIC algorithm estimates the source locations by sifting out the field points at which the peaks of MUSIC power occur. The MUSIC power at a trial field point is defined by

$$P_M = \frac{1}{\sum_{n=N+1}^{M} |\hat{\mathbf{a}}^H \mathbf{v}_n|^2}, \tag{11}$$

where $\hat{\mathbf{a}}$ is the vector of Green's functions between the reference microphones and trial field points. A trial field point indicates an assumed source location. When the vector $\hat{\mathbf{a}}$ is equal to the vector $\hat{\mathbf{g}}_i$, the quantities inside the summation of Eq. (11) become zero, and the value of the MUSIC power becomes infinitely large. In practice, due to the finite number of samples, the value of the MUSIC power at the source position remains finite but still significantly larger than the MUSIC power values at the adjacent points.

In practice, in order to find the vectors that lead to large MUSIC powers, an $l \times l$ grid was constructed at the source plane and used to calculate the power for $l \times l$ trial points. The points obtained in this way resulted in large values of MUSIC power that represented locations of the sources. The finer the grid becomes, the more conspicuously the peaks of the MUSIC power distribution stand out. However, the computational time required to calculate the power for all trial vectors also increases as the number of grid points increases. In order to identify the location of sources more efficiently, the local maximum areas are first determined approximately using a coarse grid, and referred locations of the sources can then be found by using the steepest descent algorithm based on a finer grid near the local maximum.

If the sources are not monopole-like ones, i.e., distributed sources, high-order beam steering vectors must be used in order to obtain better results. Although the beam steering vector used in this paper is limited to the type corresponding to monopole-like sources, the fifth simulation described in Section 3 shows that the method may also be applicable for distributed sources with reasonable accuracy and efficiency.

2.2. Source signal estimation via beamforming

In order to separate the source signals from the reference microphones, beamforming algorithms such as the Minimum Variance (MV) method and the Adaptive Nulling method can be employed. Although those two algorithms give similar results for compact sources, it is shown later in the fifth simulation that the Adaptive Nulling algorithm reproduces the distributed source signals better than the MV method. Therefore, the main focus of this paper is on the Adaptive Nulling method. Good overviews of the MV method are provided in many references [15,16] and also briefly presented in Appendix C.

2.2.1. Adaptive nulling algorithm

In the Adaptive Nulling algorithm, a beam steering vector that satisfies the twin conditions that the inner product with the desired direction is maximized while the gain along the undesired direction at zero is maintained is found. That is,

$$\text{maximize} |\mathbf{a}_i \cdot \hat{\mathbf{g}}_i|, \tag{12}$$

$$\text{subject to } ||\mathbf{a}_i|| = 1, \tag{13}$$

$$\mathbf{a}_i \cdot \hat{\mathbf{g}}_j = 0 \quad \text{for} \quad i \neq j. \tag{14}$$

The solution to the optimization problem represented by Eqs. (12)–(14) is efficiently obtained by utilizing the orthogonal properties of eigenvectors with respect to each other. Consider a linear array of M reference microphones that receive signals from $N-1$ incoherent sources skipping assumed to be desired ith source signal. The number of reference measurements is larger than $N-1$. The complementary Green's function

matrix then becomes

$$\hat{\mathbf{G}}_i = \begin{bmatrix} \hat{\mathbf{g}}_1 & \cdots & \hat{\mathbf{g}}_{i-1} & \hat{\mathbf{g}}_{i+1} & \cdots & \hat{\mathbf{g}}_N \end{bmatrix}, \tag{15}$$

The complete SVD of $\hat{\mathbf{G}}_i$ becomes

$$\hat{\mathbf{G}}_i = \mathbf{Q}_1 \mathbf{\Lambda} \mathbf{Q}_2, \tag{16}$$

where the columns of $\mathbf{Q}_1(M \text{ by } M)$ are the eigenvectors of $\hat{\mathbf{G}}_i \hat{\mathbf{G}}_i^{\mathrm{T}}$, the column of $\mathbf{Q}_2(N-1 \text{ by } N-1)$ are the eigenvectors of $\hat{\mathbf{G}}_i^{\mathrm{T}} \hat{\mathbf{G}}_i$, and the singular values on the diagonal of $\Lambda(M \text{ by } N-1)$ are the square roots of the nonzero eigenvalues of both $\hat{\mathbf{G}}_i \hat{\mathbf{G}}_i^{\mathrm{T}}$ and $\hat{\mathbf{G}}_i^{\mathrm{T}} \hat{\mathbf{G}}_i$

The matrix $\hat{\mathbf{G}}_i$ can be spanned by the $N-1$ left singular vectors since the rank is at most $N-1$. Therefore, the Green's function for the signals excluding the desired signal $\hat{\mathbf{g}}_j$ can be represented as

$$\hat{\mathbf{g}}_j = \sum_{k=1}^{N-1} \alpha_k \mathbf{e}_k, \tag{17}$$

where $\mathbf{e}_k$ is the kth left singular vector of the complementary Green's function matrix $\hat{\mathbf{G}}_i$, and α_k is a complex constant. If the beam steering vector $\mathbf{a}_i$ is represented as a linear combination of the other remaining singular vectors, i.e., as

$$\mathbf{a}_i = \sum_{k=N}^{M} \alpha_k \mathbf{e}_k, \tag{18}$$

Eq. (14) can be satisfied by the orthogonal properties of eigenvectors with respect to each other. That is,

$$\mathbf{a}_i \cdot \hat{\mathbf{g}}_j = \left(\sum_{k=N}^{M} \alpha_k \mathbf{e}_k \right) \cdot \left(\sum_{k=1}^{N-1} \alpha_k \mathbf{e}_k \right) = 0 \quad \text{for } i \neq j. \tag{19}$$

By using the representation of Eq. (19), Eqs. (12) and (13) become, respectively,

$$\left\| \sum_{k=N}^{M} \alpha_k \mathbf{e}_k \right\| = 1, \tag{20}$$

$$\mathbf{a}_i \cdot \hat{\mathbf{g}}_i = \sum_{k=N}^{M} \alpha_k \mathbf{e}_k \cdot \hat{\mathbf{g}}_i = \sum_{k=N}^{M} \alpha_k g_k^e = \boldsymbol{\alpha} \cdot \mathbf{g}^e. \tag{21}$$

Here, g_k^e is a complex constant from the inner product $\mathbf{e}_k \cdot \hat{\mathbf{g}}_i$ and $\boldsymbol{\alpha}$ and $\mathbf{g}^e$ are the vector notation for the complex constants α_k and g_k^e, respectively. The multiplication on the right hand side of Eq. (21) is maximized when the two vectors $\boldsymbol{\alpha}$ nd $\mathbf{g}^e$ are parallel. Hence, the expansion coefficient $\boldsymbol{\alpha}$ can be represented as

$$\boldsymbol{\alpha} = [g_N^e \quad \cdots \quad g_M^e]^{\mathrm{T}}. \tag{22}$$

In conclusion, the beam steering vector for the ith source can be obtained as

$$\mathbf{a}_i = \frac{\sum_{k=N}^{M} g_k^e \mathbf{e}_k}{\left\| \sum_{k=N}^{M} g_k^e \mathbf{e}_k \right\|}. \tag{23}$$

By using the obtained beam steering vector, the individual source signals can be estimated by the following procedure:

$$\begin{aligned} q_i &= \mathbf{a}_i \cdot \mathbf{r} = \mathbf{a}_i \cdot [\hat{\mathbf{g}}_1 \quad \cdots \quad \hat{\mathbf{g}}_N]\mathbf{s} \\ &= \begin{bmatrix} 0 & \cdots & 0 & \mathbf{a}_i \cdot \hat{\mathbf{g}}_i & 0 & \cdots & 0 \end{bmatrix} \mathbf{s} \\ &= c_i s_i. \end{aligned} \tag{24}$$

Here, q_i is the estimated source signal of s_i denoted as a complex constant $c_i s_i$, and $\hat{\mathbf{g}}_i$ is the Green's function between the reference microphones and the ith source. Thus, once the beam steering vector is obtained, we can

estimate the source signal by just multiplying the vector by the reference array response. The other source signals can also be estimated in a similar manner.

2.2.2. Modified adaptive nulling algorithm for distributed sources

The beamforming procedures derived in the previous Section 2.2.1 are suited to compact sources or far-field problems where sound sources can be regarded as point sources. In order to obtain uncontaminated individual source signals, the influence of undesired source signals is removed by applying the beam vector that causes the gain along the undesired direction to become zero. For distributed sources or near-field applications, a modified beam vector that maintains the gain along the several directions of the source area as zero is necessary.

It would be possible to consider an effective boundary that may be defined as the contours of the half power points of the MUSIC power distribution. When the radius of the effective boundary for a distributed source s_j is denoted by δ_j, gains from the three points of the estimated source (i.e., the center and the two opposite points on the effective boundary of the source areas) must be zero:

$$\mathbf{a}_i \cdot [\,\hat{\mathbf{g}}_j^{-\delta_j} \quad \hat{\mathbf{g}}_j \quad \hat{\mathbf{g}}_j^{+\delta_j}\,] = [0\ 0\ 0] \quad \text{for } i \neq j, \tag{25}$$

where $\hat{\mathbf{g}}_j^{-\delta_j}$ and $\hat{\mathbf{g}}_j^{+\delta_j}$ are the geometrical transfer functions (Green's functions) of the boundary from the estimated jth source locations to the reference array. Then, the alternative Green's function matrix of Eq. (15) becomes

$$\tilde{\hat{\mathbf{G}}}_i = \left[\hat{\mathbf{g}}_1 \quad \cdots \quad \hat{\mathbf{g}}_{i-1} \quad \hat{\mathbf{g}}_{i+1} \quad \cdots \quad \hat{\mathbf{g}}_j^{-\delta} \quad \hat{\mathbf{g}}_j \quad \hat{\mathbf{g}}_j^{+\delta} \quad \cdots \quad \hat{\mathbf{g}}_N\right]. \tag{26}$$

The modified beam steering vector is obtained by the same procedure as in Eqs. (18)–(23) by using $N+2$ instead of N with Eqs. (25) and (26). Since the rank of $\tilde{\hat{\mathbf{G}}}_i$ is $N+1$, the number of reference measurements should be larger than $N+1$ to span the beam steering vector with eigenvectors as in Eq. (19). Although the exact area of near-field sources may not be clearly identified by the MUSIC method itself, the proposed method gives better results than the original nulling method and conventional methods since the effect of the cross-talk is reduced sufficiently. The details will be shown in the fifth simulation results of Section 3.

2.3. Reconstruction of partial field

The measured field signal vector $\mathbf{y}_h$ may be expressed in terms of the estimated source signal vector $\mathbf{q}$ and the transfer function matrix $\mathbf{H}$:

$$\mathbf{y}_h = [\mathbf{h}_1 \quad \cdots \quad \mathbf{h}_N] \begin{bmatrix} q_1 \\ \vdots \\ q_N \end{bmatrix} + \mathbf{n} = \mathbf{H}\mathbf{q} + \mathbf{n}, \tag{27}$$

where $\mathbf{h}_j$ is the transfer function vector between the ith source signal q_i and field microphone measurements, and $\mathbf{n}$ is the measurement noise vector. Since $\mathbf{q}$ is available and $\mathbf{y}_h$ is the measured values, $\mathbf{H}$ can be obtained deterministically by solving Eq. (27) in least square sense. Once the transfer function matrix has been determined, the ith partial pressure vector $\mathbf{y}_h^i$ can be calculated as

$$\mathbf{y}_h^i = q_i \mathbf{h}_i. \tag{28}$$

For the d times of measurements, the magnitude and phase of the ith partial pressure at the kth field point can be computed by taking the ensemble average:

$$|y_k^i|^2 = \frac{1}{d}\sum_{j=1}^{d} (h_{k,i}q_i)_j^* (h_{k,i}q_i)_j, \tag{29}$$

$$\theta(y_k^i) = \text{phase}\left\{\frac{\sum_{j=1}^{d}(h_{k,i}q_i)_j^*(q_i)_j}{\sum_{j=1}^{d}(q_i)_j^*(q_i)_j}\right\}, \tag{30}$$

where $h_{k,j}$ is the kth element of $\mathbf{h}_i$. Note that the solution does not depend on the statistical properties of sources any longer, which makes the solution much robust to noise. Each partial field on the hologram plane can then be reconstructed by getting partial pressures in each measurement point in the same way.

3. Simulation results and discussion

Five different cases of simulation studies have been conducted to evaluate the performance of the proposed method at 800 Hz. The configuration for the simulations is shown in Fig. 1, and the simulation conditions for each case are presented in Table 1. Two incoherent point sources, A and B, represented by independent random signals are located at (−0.15, 0 m) and (0.15, 0 m) on the source plane, respectively. The grids on the source plane are 32×32, the spacing is 0.025 m both in the x- and y-directions, and they are used to calculate the trial vectors of MUSIC power for estimating the source location. The reference array is composed of eight points (microphones) spaced 0.08 m apart in the x-direction on a reference plane which is located at a distance $z_r = 0.05$, 0.15 and 0.5 m from the source plane, depending on each simulation as shown in Table 1. The hologram plane at a distance $z_h = 0.10$ m from the source plane is divided into 16×16 points spaced 0.05 m in the x- and y-directions. The pressure values at each microphone position are calculated by using Green's functions and averaged 64 times. Particularly, the exact partial pressures for each source are calculated on the assumption that only one corresponding source is on. Note that in the simulations of conventional methods, the two points closest to each source among the eight references (i.e., the third and sixth references from the left-hand side) are used as reference microphone positions. The results of partial fields obtained from each simulation are compared to the exact values on the x-axis of the hologram plane.

Through the simulations, MUSIC power distributions are first calculated for all the grids on the source plane to determine the source locations. Fig. 2 shows the MUSIC power distributions for the first simulation. Two clear, dominant peaks are shown in the MUSIC power distribution and the source locations can be determined by finding the positions of those local maxima. In the following simulations, the source locations could be determined in the same way and the results were good enough regardless of various simulation conditions. Hence, MUSIC results for the other simulation cases are not shown in this paper.

The first and second cases of simulations were designed to illustrate the effect of the reference locations on the partial field reconstruction. For the first simulation case in which the reference plane is located 0.05 m from source plane, the results of each partial field obtained by using the present and conventional methods are compared with the exact results in Fig. 3. It may be seen that for the present method the decomposed partial

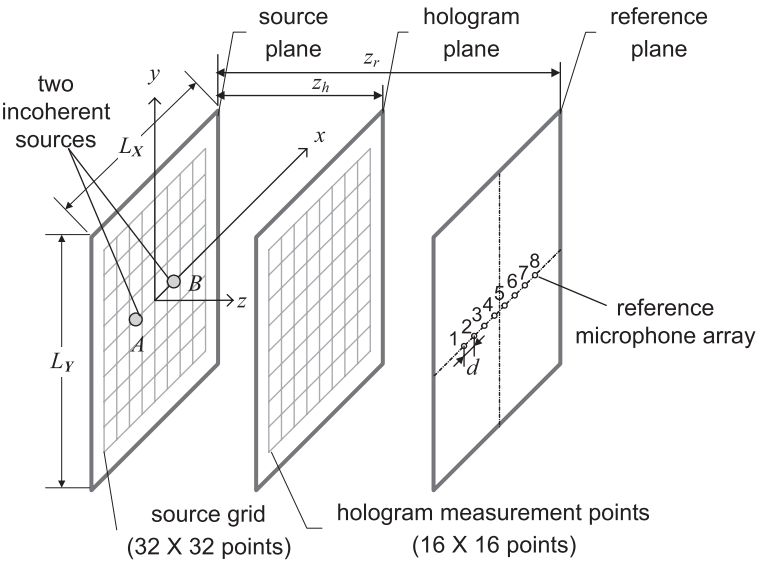

Fig. 1. Configuration for numerical simulations.

Table 1
Conditions for numerical simulation cases

Simulation cases	Sources	Distance from source plane to reference plane, Z_r (m)	S/N ratio (dB)	Relative source level (dB)
Case 1	Two incoherent point sources are	0.05	30	0
Case 2	0.30 m apart from each other	0.5	30	0
Case 3		0.05	12	0
Case 4		0.05	30	12
Case 5	Distributed sources	0.15	30	0

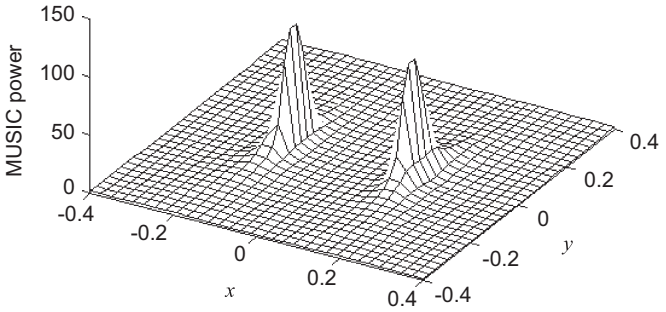

Fig. 2. MUSIC power distribution for two incoherent point sources at 800 Hz in simulation case 1.

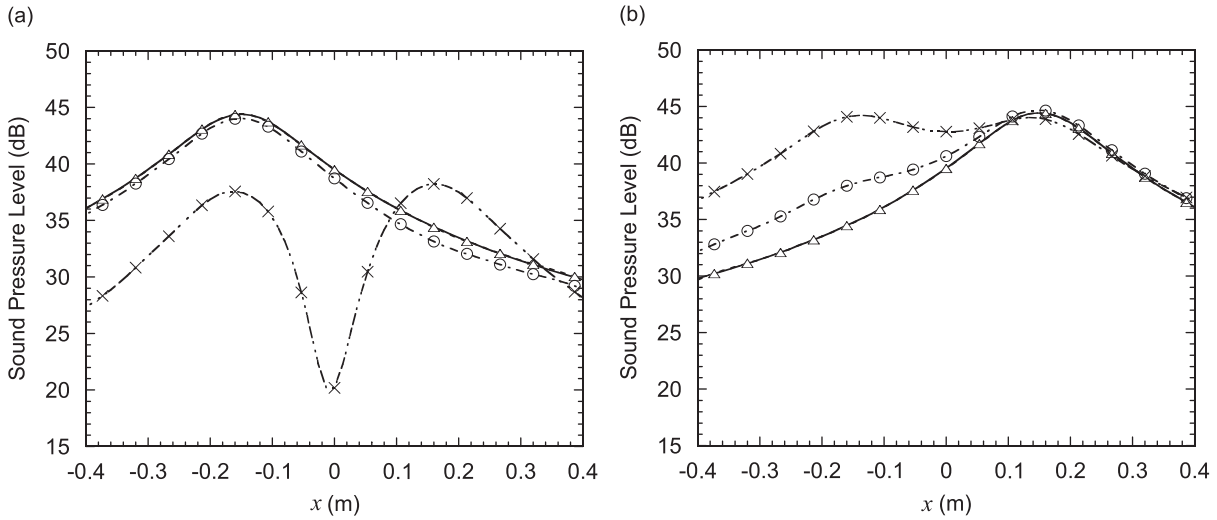

Fig. 3. Results of simulation case 1: decomposed partial fields on x-axis of hologram plane for (a) source A and (b) source B. ——, exact; – △ –, beamforming method; — ○—, partial coherence method; —×– –, SVD method.

fields are almost equal to the exact partial fields. However, for the partial coherence method, the effects of cross-talk from the other source signals are visible in both partial fields although each reference was very close to the corresponding sources. The SVD method provides considerably different results from the exact partial fields: i.e., the partial fields of the sources cannot appear to be decomposed at all. In the second simulation case, the reference array was located 0.50 m from the source plane, which is ten times farther compared to the first case. It may be seen from Fig. 4 that both the conventional methods give poor results, while the present method provides reasonably good results compared the exact partial fields. From the first and second

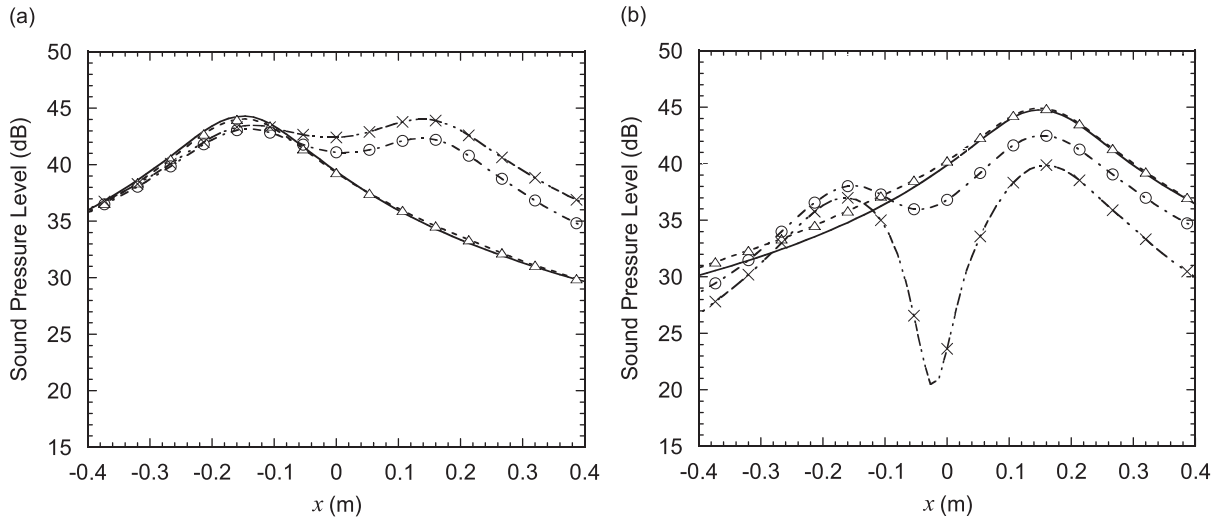

Fig. 4. Results of simulation case 2: decomposed partial fields on x-axis of hologram plane for (a) source A and (b) source B. ———, exact; – △– ·, beamforming method; — ○—, partial coherence method; —×· –, SVD method.

simulations, it may be concluded that the beamforming technique is more robust with respect to the positions of reference microphones than conventional methods.

The third simulation shows how well the proposed algorithm performs when the signals are measured in noisy conditions, in this case 12 dB S/N ratio. The signal-to-noise ratio is defined in decibels (dB) by (S/N ratio) $= 10\log_{10}(\psi_s^2/\psi_n^2)$, where ψ_s is the rms value of the signal that can be acquired without significant distortion, and ψ_n is the rms value of the data acquisition system noise floor. In general, measurements are performed in anechoic environments, and hence a 12 dB S/N ratio may be a very harsh condition. As may be seen in Fig. 5, the decomposed partial fields obtained via the proposed method are found to be in good agreement with the exact partial pressures. Note also that the conventional methods are not sensitive to noise as may be found by comparing Figs. 3 and 5.

The fourth simulation was made to illustrate performances of the methods under the condition that the two incoherent sources have very different sound pressure levels: a 12 dB difference in levels was assumed in this case. In Fig. 6, it may be seen that the present method offered a complete decomposition of the partial fields while the other methods could not distinguish two sources having relatively large level differences. Thus it may be said that the proposed method can reconstruct more complex sound fields very efficiently.

In the fifth simulation case, the effect of distributed source was investigated while the point sources were assumed in the previous simulations. In general, distributed sources are modeled by using several coherent point sources in numerical simulations. In this study, each distributed source was represented by three point sources that are located 0.05 m apart from each other as may be seen in Fig. 7. It was assumed that the phases of the two outer sources were 180° out-of-phase from the source located at the center point and that the magnitudes of the three point sources were equal. Since the conventional methods did not give good results for the point sources in the previous simulation cases, other beamforming algorithms such as MV, direct inverse and modified adaptive nulling methods are considered in this case. At first, each partial field was reconstructed by using the original adaptive nulling method in the same way as in the previous cases. As shown in Fig. 8, the original adaptive nulling method could not offer good results any longer, due to the interference of other source signals. Next, partial fields have been obtained by the direct inverse method which directly solves Eq. (D.1) in least squares sense as described in Appendix D. However, the reconstructed partial fields include considerable errors as shown in Fig. 8 since the reference signals for the distributed sources cannot be represented by Green's functions in Eq. (D.1). The MV method has also approximated the partial fields of the distributed sources poorly. One of the reasons for the errors is that the power in Eq. (C.1) could be minimized in different directions since the Green function vector $\hat{\mathbf{g}}_i$ in Eq. (C.3) is not identical with that of the distributed sources. Finally, the modified adaptive nulling method, i.e., Eqs. (25) and (26) was used to obtain the partial

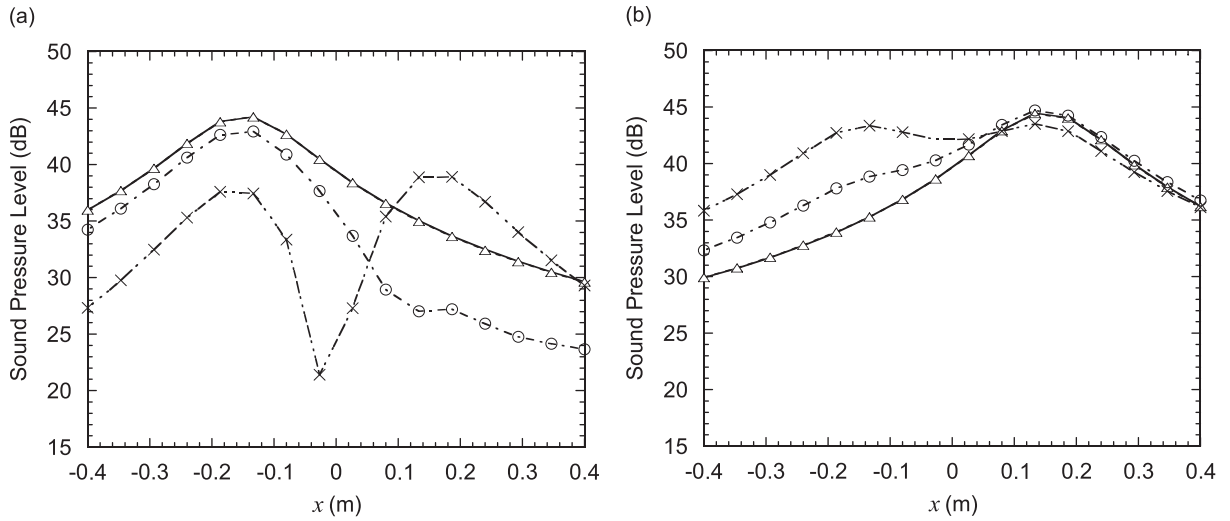

Fig. 5. Results of simulation case 3: Decomposed partial fields on x-axis of hologram plane for (a) source A and (b) source B. ——, exact; – △– ·, beamforming method; — ○—, partial coherence method; —×· –, SVD method.

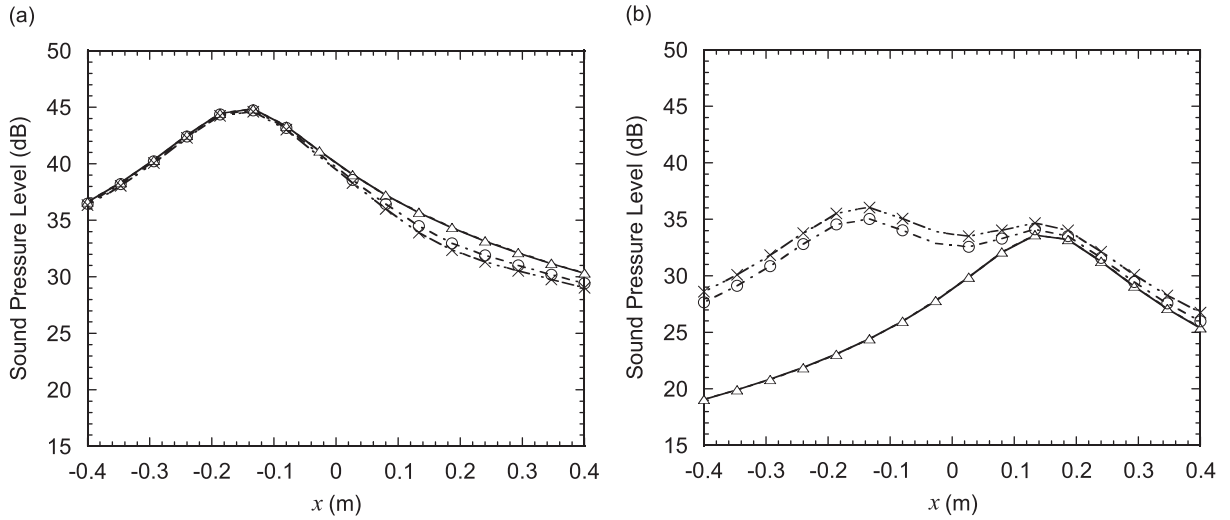

Fig. 6. Results of simulation case 4: Decomposed partial fields on x-axis of hologram plane for (a) source A and (b) source B. ——, exact; – △– ·, beamforming method; — ○—, partial coherence method; —×—, SVD method.

fields. Particularly, the radius of the effective boundary δ_j was determined to be 0.04 m from the half-power points of MUSIC power as previously described in Section 2.2.2. By removing the signals from the three points over the effective boundary as shown in Eq. (25), the interference from the other source signal is considerably reduced, and the estimated partial fields becomes very close to the exact values especially near the corresponding sources as shown in Fig. 8. Although the reconstructed partial fields may be subject to interferences to a certain degree, they are in good agreement with the exact partial fields. For various radii of the effective boundary, in particular, for those between 0.02 and 0.06 m, errors between the reconstructed and exact partial fields were found to be within 3 dB. Thus it may be said that the proposed method can be extended to the modified adaptive nulling method for partial field reconstructions of distributed sources.

All the simulation results in this section have shown that the proposed method performs very effectively at 800 Hz under various conditions. However, it should be noted that the beamforming method will not be

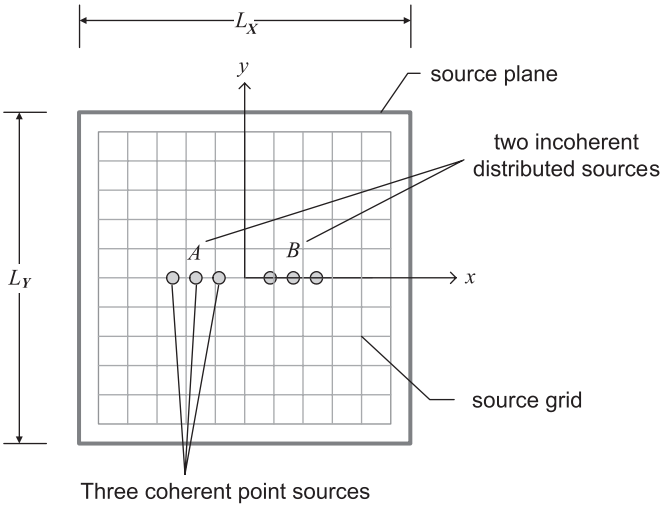

Fig. 7. A schematic of two distributed sources. Each distributed source A and B are, respectively, modeled by three coherent point sources in the fifth simulation.

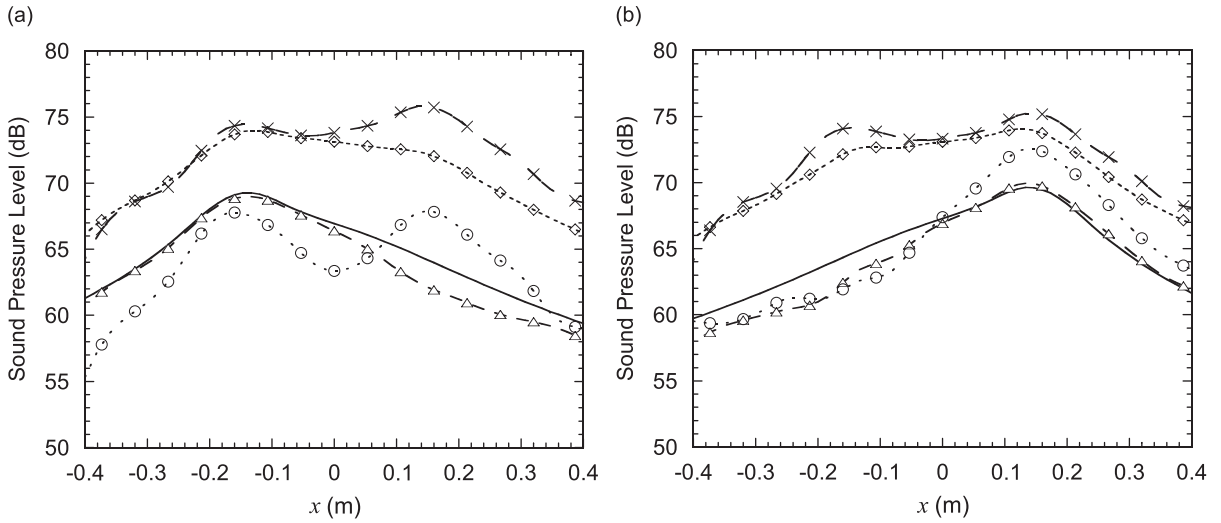

Fig. 8. Results of simulation case 5: Decomposed partial fields on x-axis of hologram plane for (a) source A and (b) source B. ———, exact; – △ –, modified adaptive nulling; — ○—, original adaptive nulling; —×—, minimum variance; ····◇····, direct inverse.

independent of the frequency since MUSIC and Adaptive Nulling algorithms used in the method depend on the frequency. At much lower frequencies, it might fail to decompose into each partial field accurately. This matter will be covered in a forthcoming work.

4. Experimental results and discussion

Two kinds of experiments were conducted at 800 Hz to demonstrate the effectiveness of the proposed method and to verify the results discussed in Section. 3. The experimental setup within a semi-anechoic chamber is shown in Fig. 9. Two loudspeakers having a diameter of 0.10 m were placed at (−0.15, 0 m) and (0.15, 0 m) on the source plane. The loudspeakers were driven by mutually incoherent random signals that were generated from LMS SCADAS III source module and amplified by two power amplifiers, Inkel AX 7030G. The reference microphone array consisted of a horizontal line array of eight B&K type 4196

microphones with spacing 0.08 m in the x-direction, which were located at either 0.05 m or 0.50 m from the source plane in the z-direction. The hologram microphone array at $z = 0.1$ m consisted of a horizontal line array of eight B&K type 4196 microphones spacing 0.05 m. The hologram array was traversed at 16 vertical positions with a uniform spacing of 0.05 m for both the left and right half-planes, respectively, to make 16×16 measurement grid. Time signals of the sound pressures measured at each microphone were recorded by a 16 channel data acquisition main frame (SCADAS III) and workstation as shown in Fig. 9. During each scanning procedure, the time signals from the hologram and reference microphones were recorded 24 times, each measurement time was 1 s, and the record length was 8192 points. For the post processing, the recorded time signals were converted to the frequency domain by Fast Fourier Transform (FFT). The FFT size and frequency resolution were 8192 and 1 Hz, respectively. For each experiment, the sound pressures on the hologram plane due to only one source were also measured by turning off the other source.

In the first experiment, the references were located 0.05 m from the source plane as in the first numerical case. After determining the rank of the reference cross-spectral matrix to be two from the measured reference signals, the MUSIC powers were calculated as shown in Fig. 10. The source locations could then be determined from the local maximum positions of the results. Next, the source signals were calculated using the original nulling method and partial fields were obtained deterministically. Compared to the simulation results, the decomposed partial fields from those signals contained a great deal of interference. The reason is that the loudspeakers used in the experiments are not compact sources. Thus the modified nulling algorithm was applied again and the partial fields were reconstructed in the same way. The effective radius was determined to be 0.05 m by the half-power points of the MUSIC power. The measured data were also processed using the conventional methods to obtain the partial fields. The references used in the conventional methods were the

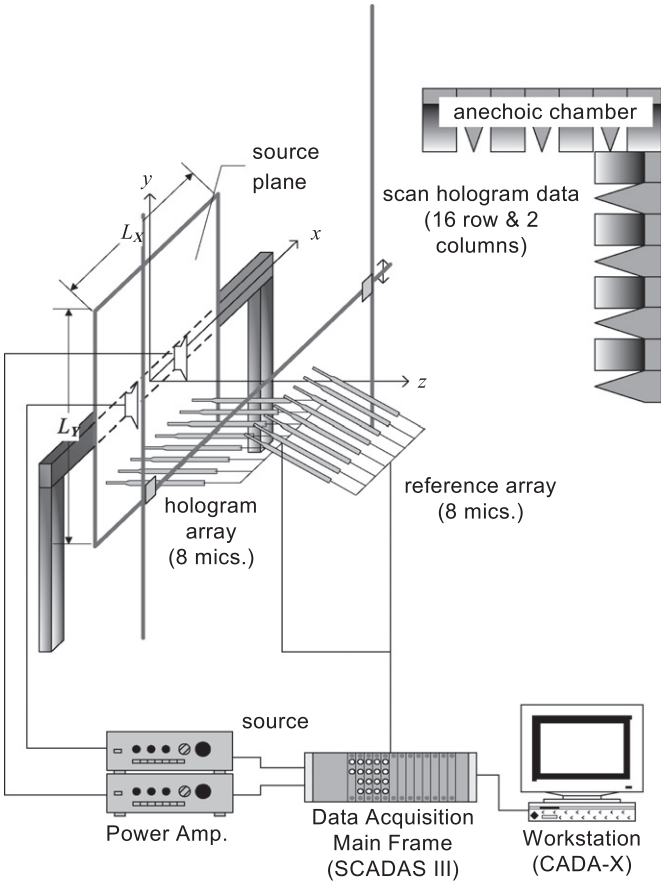

Fig. 9. Experimental setup for partial field decomposition.

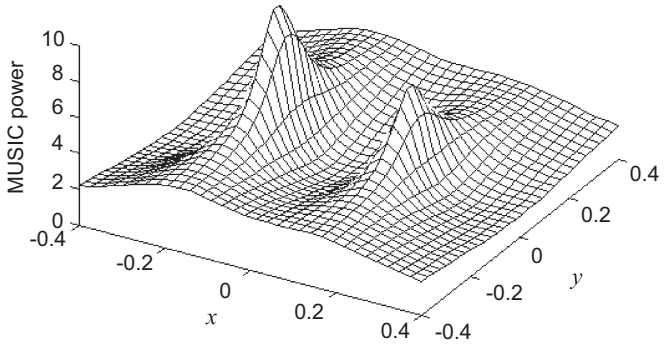

Fig. 10. Experimental results of MUSIC powers for two loudspeakers at 800 Hz.

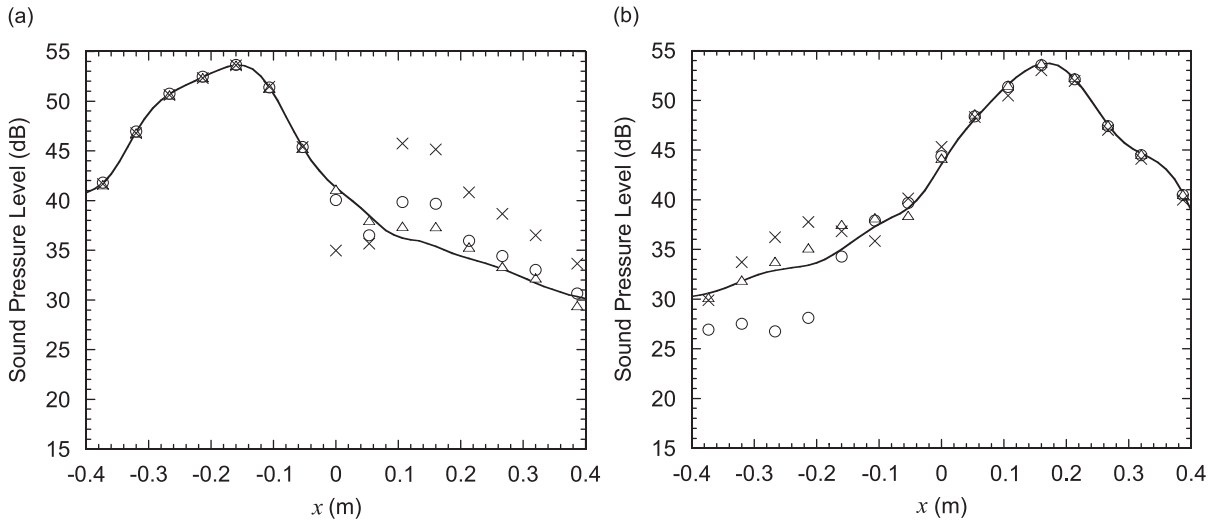

Fig. 11. Experimental results when the reference array is located 0.05 m from the source plane: decomposed partial fields on x-axis of hologram plane for (a) source A and (b) source B. ——, measured; △, beamforming method; ○, partial coherence method; ×, SVD method.

third and sixth microphones in the reference array. The selected references have strong one-to-one relationships with the corresponding source signal since their locations were very close to each source. Fig. 11 shows the decomposed partial fields obtained using the present and conventional methods. The decomposed partial fields obtained by using the proposed and the partial coherence methods are in good agreement with the measured partial fields although the results of the partial coherence method show some differences where $x > 0.1$ m for source A and $x < -0.2$ m for source B. Those from the SVD method are poor, as expected.

In the second experiment, the references were located 0.50 m from the source plane. The MUSIC powers were calculated, and the locations of the maximum values were found to be in good agreement with the positions of the physical sources even though the references were located far from the source plane. Although the peaks of the MUSIC power are less clear than those in the first experiment, they appear in the expected positions. By the same procedures mentioned above, partial fields were constructed using the proposed and conventional methods. In this experiment, the whole reference set is influenced by both of the incoherent sources up to almost the same level. Therefore, the selected references no longer have one-to-one relationships to each source signal. As may be seen in Fig. 12, while the decomposed partial fields from the conventional methods include a considerable amount of contamination, the decomposed partial fields obtained using the proposed method represents each partial field very well.

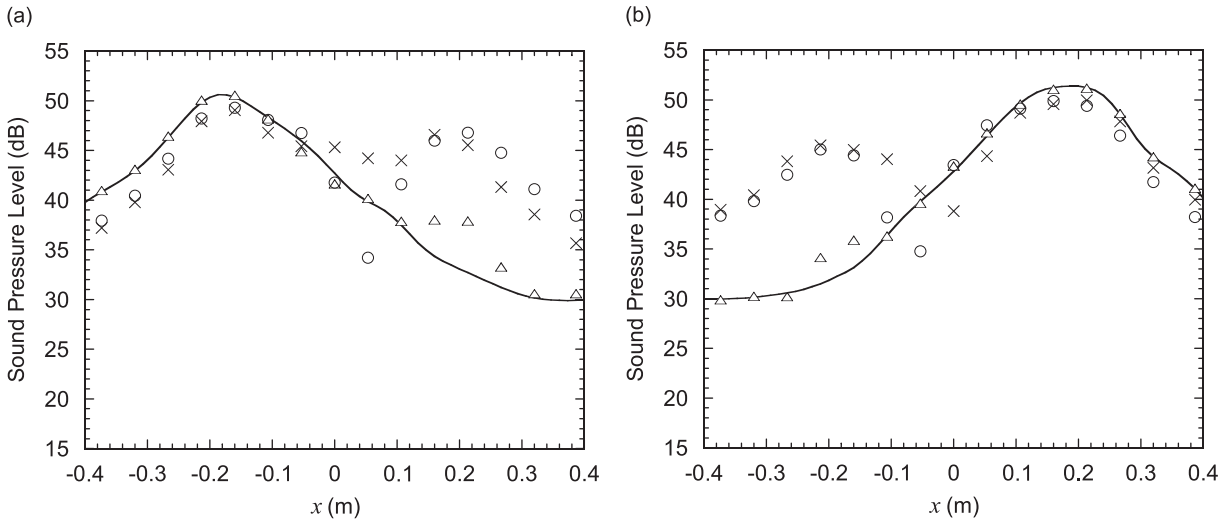

Fig. 12. Experimental results when the reference array is located 0.5 m from the source plane: decomposed partial fields on x-axis of hologram plane for (a) source A and (b) source B. ——, measured; △, beamforming method; ○, partial coherence method; ×, SVD method.

In those experiments, the locations of source candidates were determined successfully by the peaks of the MUSIC powers, even in the absence of restrictions on the locations of the reference microphones. By applying beamforming to the obtained source locations, each source signal was estimated, and using the estimated source signals the composite pressures were decomposed into partial pressures deterministically. From the results of the two experiments, the proposed partial field decomposition method was found to work more efficiently than the conventional methods even in the absence of restrictions on the locations of the reference microphones.

As a supplement, in order to identify sources, the partial pressures in the source plane were reconstructed by applying NAH to each decomposed partial field in the second experiment. The reconstructed partial pressures in the source plane are presented as contour plots where the lines represent contours of equal levels. Figs. 13(a) and (b) are the results of the proposed method and clearly show each loudspeaker at the expected location. However, the results obtained using the partial coherence method for one source are contaminated by the other source signal as shown in Figs. 13(c) and (d). Thus the predicted partial pressures obtained by using the conventional method fail to clearly identify the two incoherent loudspeaker sources.

5. Conclusions

In order to identify sound sources from a sound field that is generated by multiple incoherent sources, a new partial field decomposition method based on beamforming has been proposed. It has been demonstrated that both source locations and signals can be estimated accurately by using beamforming. It has also been shown that from the calculated signals the measured pressures can be decomposed into partial pressures, deterministically. Numerical simulations have confirmed good performances of the proposed method in various conditions. Finally, experiments have also showed that the proposed method can be applied to truly distributed sources and gives good results even in the absence of restrictions on the locations of the reference microphones.

Acknowledgments

The first author would like to thank Dr. Young Man Cho, who was a close colleague in my department, for his valuable and helpful discussions. The authors would also like to thank the referees for their valuable

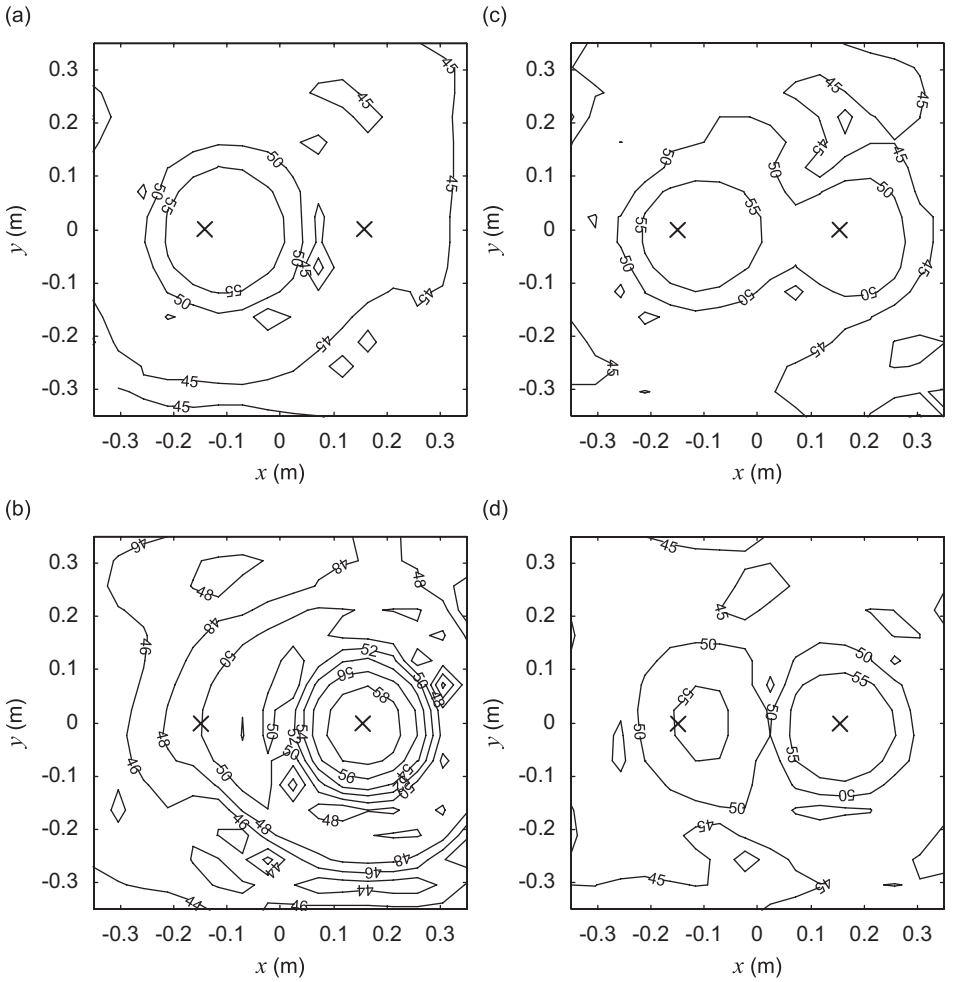

Fig. 13. Comparison of sets of partial fields located on the source plane reconstructed from the sets of decomposed partial fields when the reference array is located 0.5 m from the source plane: (a), (b) present method and (c), (d) partial coherence method. The mark " × " denotes the center position of actual sources.

suggestions, comments and constructive criticism. This work was supported by the Brain Korea 21 Project of the Ministry of Education in Korea and the IAMD at Seoul National University.

Appendix A. Singular value decomposition (SVD) method

In the SVD-based partial field decomposition method, the auto-spectrum S_{yy} of the signal of a field point on a hologram plane can be represented by the reference cross-spectrum and corresponding transfer function:

$$S_{yy} = \mathbf{H}^H \mathbf{S}_{rr} \mathbf{H} + \sigma_n^2, \tag{A.1}$$

where $\mathbf{H}$ is the transfer vector between the references and a field point at the hologram plane, $\mathbf{S}_{rr}$ is the cross-spectral matrix of the references, σ_n^2 is the measurement noise and the superscript H represents the Hermitian transpose. The SVD of $\mathbf{S}_{rr}$ in Eq. (6) leads to

$$\mathbf{S}_{rr} = \mathbf{V}(\mathbf{\Lambda} + \sigma_n^2 \mathbf{I})\mathbf{V}^H, \tag{A.2}$$

where $\mathbf{\Lambda}$ is a diagonal matrix of the singular values and $\mathbf{V}$ is an associated square orthonormal matrix of the singular vectors, and σ_n^2 is the variance of the background and measurement noise. Assuming that reference

signals are strongly related to real source signals,

$$\mathbf{S}_{rr} \approx \mathbf{V}\mathbf{\Lambda}\mathbf{V}^H. \tag{A.3}$$

Substitution of Eq. (A.3) into Eq. (A.1) gives

$$S_{yy} = \hat{\mathbf{H}}^H \mathbf{\Lambda} \hat{\mathbf{H}} + \sigma_n^2, \tag{A.4}$$

where $\hat{\mathbf{H}} = \mathbf{V}^H\mathbf{H}$ is the estimated transfer vector. It should be noted that the singular values and their corresponding singular vectors are assumed to represent mutually incoherent sources. The set of partial fields can then be represented as

$$y_i = \mathbf{H}^H \mathbf{v}_i \lambda_i^{1/2}, \tag{A.5}$$

where y_i is the contribution from the ith partial source at the field point, λ_i is the ith element of the decomposed diagonal matrix, and $\mathbf{v}_i$ is the ith column of the decomposed orthonormal matrix. Partial fields are then constructed from those contributions of the whole holograms. Although the obtained singular vectors are orthogonal with respect to each other, the singular vectors are generally different from the response vectors of the exact source signals at the reference microphones. It is not uncommon for the two vectors to be only weakly related. The effectiveness of partial field decomposition is completely dependent on a strong relation between the reference and source signal vectors which cannot be ensured on a consistent basis.

Appendix B. Partial coherence method

Whenever there is a reference microphone near each source, each source signal can be represented approximately by the corresponding microphone measurement. Such an observation leads to the partial coherence method, whereby the partial field is obtained by finding the portion of the pressure signal on the hologram plane that is coherent with the corresponding reference signal. The first partial field is obtained from the contribution of the first reference signal:

$$y_1 = \frac{S_{r_1 y}}{(S_{r_1 r_1})^{1/2}}, \tag{B.1}$$

where $S_{r_1 y}$ is the cross-spectrum of the first reference signal and a field point signal, and $S_{r_1 r_1}$ is the auto-spectrum of the first reference signal.

The second partial field is then obtained from the contribution of the conditioned second reference signal:

$$y_2 = \frac{S_{r_2 y \cdot r_1}}{(S_{r_2 r_2 \cdot r_1})^{1/2}}, \tag{B.2}$$

where $S_{r_2 y \cdot r_1}$ is the cross-spectrum between the second reference signal and a field point signal, and $S_{r_2 r_2 \cdot r_1}$ is the auto-spectrum of the second reference signal after the linear effects of the first reference signal is removed from each signal. They can be represented as

$$S_{r_2 y \cdot r_1} = S_{r_2 y} - \frac{S_{r_2 r_1} S_{r_1 y}}{S_{r_1 r_1}} \tag{B.3}$$

and

$$S_{r_2 r_2 \cdot r_1} = S_{r_2 r_2} - \frac{S_{r_2 r_1} S_{r_1 r_2}}{S_{r_1 r_1}}. \tag{B.4}$$

Here, the contamination of the q-th reference signal is removed by using the following relation:

$$S_{ij \cdot q} = S_{ij} - \frac{S_{iq} S_{qj}}{S_{qq}}, \tag{B.5}$$

where $S_{ij \cdot q}$ denotes the conditioned cross-spectrum between the ith and jth signals after the contribution of the qth signal is removed from both the ith and jth signals, and S_{ij}, S_{qq}, S_{iq} and S_{qj} denote the cross-spectra between indexed references.

However, when the reference microphones are located far from sources, a measured reference signal represents a combination of multiple source signals, which leads to poor representation of the source signals. In this case, since its performance depends on the quality of the estimated source signals, the partial coherence method fails to reconstruct the partial field. This is an undesirable limitation from a practical point of view, since the proximity of the reference microphones to the source signals cannot always be guaranteed.

Appendix C. Minimum variance (MV) method

The underlying principle of the MV method boils down to find an optimal steering vector such that the array output power is minimized while the gain along the look direction of the source of interest as unity is maintained. That is,

$$\text{minimize } \mathbf{w}_i^H \mathbf{S}_{rr} \mathbf{w}_i \tag{C.1}$$

$$\text{subject to } |\mathbf{w}_i^H \hat{\mathbf{g}}_i| = 1, \tag{C.2}$$

where $\hat{\mathbf{g}}_i$ is the Green's function vector between the references and ith source, and $\mathbf{S}_{rr}$ is the reference cross-spectral matrix. Using the Lagrangian multiplier, it can be shown that

$$\mathbf{w}_{i,\text{opt}} = \frac{\mathbf{S}_{rr}^{-1} \hat{\mathbf{g}}_i}{\hat{\mathbf{g}}_i^H \mathbf{S}_{rr}^{-1} \hat{\mathbf{g}}_i}. \tag{C.3}$$

Appendix D. Direct inverse method

By using the estimated source locations in Section 2.1, the reference signals in Eq. (5) can be approximated as

$$\mathbf{r} \approx \hat{\mathbf{G}} \mathbf{s} + \mathbf{n}, \tag{D.1}$$

where $\hat{\mathbf{G}}$ is the Green's functions matrix between the reference locations and the estimated source locations. The source signals can be estimated by directly solving Eq. (D.1) while minimizing the least square error. However, the least squares solution is highly sensitive to estimation error in $\hat{\mathbf{G}}$ as shown by the simulation study in Section 3. It should be noted that the fidelity of the least squares solution to Eq. (D.1) with distributed sources would be degraded. Because many point sources are needed to represent distributed sources, the least square error is essential.

References

[1] J.D. Maynard, E.G. Williams, Y. Lee, Nearfield Acoustical Holography: I. Theory of generalized holography and the development of NAH, *Journal of the Acoustical Society of America* 78 (4) (1985) 1395–1413.
[2] J. Hald, STSF—a unique technique for scan-based nearfield acoustical holography without restriction on coherence, *B&K Technical Review No* 1 (1988).
[3] D.L. Hallman, J.S. Bolton, Multi-reference nearfield acoustical holography, *Proceedings of Inter-Noise* 92 (1992) 1165–1170.
[4] Julius S. Bendat, Allan G. Piersol, *Random Data: Analysis and Measurement Procedures*, Wiley, New York, 2000.
[5] D.L. Hallman, J.S. Bolton, A comparison of multi-reference nearfield acoustical holography procedures, *Proceedings of Noise-Con* 94 (1994) 929–934.
[6] M.A. Tomlinson, Partial source discrimination in near field acoustic holography, *Applied Acoustics* 57 (1999) 243–261.
[7] H.S. Kwon, J.S. Bolton, Partial field decomposition in nearfield acoustical holography by the use of singular value decomposition and partial coherence procedures, *Proceedings of Noise-Con* 98 (1998) 649–654.
[8] H. Takata, T. Nishi, W. Jiang, J.S. Bolton, The use of Nearfield Acoustical Holography (NAH) and partial field decomposition to identify and quantify the sources of exterior noise radiated from vehicle, *Proceedings of SAE* 972053 (1997) 1449–1455.
[9] J. Hald, Use of spatial transformation of sound fields (STSF) techniques in the automotive industry, *B&K Technical Review* 1 (1995).
[10] R.O. Schmidt, Multiple emitter location and signal parameter estimation, *IEEE Transactions on Antennas and Propagation* AP 34 (3) (1986) 276–280.
[11] M.R. Bai, J. Lee, Industrial noise source identification by using an acoustic beamforming system, *Transactions of ASME* 120 (1998) 426–433.

[12] K.-U. Nam, Y.-H. Kim, Visualization of multiple incoherent sources by the backward prediction of near-field acoustic holography, *Journal of the Acoustical Society of America* 109 (2001) 1808–1816.
[13] K.-U. Nam, Y.-H. Kim, A partial field decomposition algorithm and its examples for near-field acoustical holography, *Journal of the Acoustical Society of America* 116 (2004) 172–185.
[14] Y.-K. Kim, J.S. Boltion, H.S. Kwon, Partial field decomposition in multi-reference near-field acoustical holography by using optimally located virtual references, *Journal of the Acoustical Society of America* 115 (2004) 1641–1652.
[15] S.U. Pillai, *Array Signal Processing*, Springer, New York, 1989.
[16] D.H. Johnson, D.E. Dudgeon, *Array Signal Processing: Concepts and Techniques*, Prentice-Hall, Englewood Cliffs, NJ, 1993.